

## Article

# Temporally and Spatially Resolved Simulation of the Wind Power Generation in Germany

Reinhold Lehneis <sup>1,\*</sup>  and Daniela Thrän <sup>1,2</sup> 

<sup>1</sup> Department of Bioenergy, Helmholtz Centre for Environmental Research GmbH—UFZ, Permoserstraße 15, 04318 Leipzig, Germany

<sup>2</sup> Bioenergy Systems Department, DBFZ Deutsches Biomasseforschungszentrum gGmbH, Torgauer Str. 116, 04347 Leipzig, Germany

\* Correspondence: reinhold.lehneis@ufz.de

**Abstract:** Temporally and spatially resolved data on wind power generation are very useful for studying the technical and economic aspects of this variable renewable energy at local and regional levels. Due to the lack of disaggregated electricity data from onshore and offshore turbines in Germany, it is necessary to use numerical simulations to calculate the power generation for a given geographic area and time period. This study shows how such a simulation model, which uses freely available plant and weather data as input variables, can be developed with the help of basic atmospheric laws and specific power curves of wind turbines. The wind power model is then applied to ensembles of nearly 28,000 onshore and 1500 offshore turbines to simulate the wind power generation in Germany for the years 2019 and 2020. For both periods, the obtained and spatially aggregated time series are in good agreement with the measured feed-in patterns for the whole of Germany. Such disaggregated simulation results can be used to analyze the power generation at any spatial scale, as each turbine is simulated separately with its location and technical parameters. This paper also presents the daily resolved wind power generation and associated indicators at the federal state level.

**Keywords:** wind turbines; reanalysis weather data; wind energy; spatiotemporal modeling



**Citation:** Lehneis, R.; Thrän, D. Temporally and Spatially Resolved Simulation of the Wind Power Generation in Germany. *Energies* **2023**, *16*, 3239. <https://doi.org/10.3390/en16073239>

Academic Editor:  
Francesco Castellani

Received: 23 February 2023  
Revised: 29 March 2023  
Accepted: 1 April 2023  
Published: 4 April 2023



**Copyright:** © 2023 by the authors. Licensee MDPI, Basel, Switzerland. This article is an open access article distributed under the terms and conditions of the Creative Commons Attribution (CC BY) license (<https://creativecommons.org/licenses/by/4.0/>).

## 1. Introduction

Renewable energy from wind turbines can significantly reduce the global demand for conventional energy sources, and thus plays a key role in decarbonizing the electricity sector, promoting both national independence from fossil fuels and climate protection. Over the past decade, wind energy has experienced a remarkable upswing worldwide, supported by a steady decline in the levelized cost of electricity. Nearly 94 GW of new wind turbine capacity was installed globally in 2021, including 21 GW offshore, leading to a total capacity of 837 GW [1]. In Germany, the installed onshore capacity rose from 26.8 GW in the year 2010 to 56.1 GW at the end of 2021 [2]. At the same time, the offshore capacity increased from 80 MW to 7.8 GW [2]. Against the backdrop of the current energy and climate crisis, the German government's latest amendment to the Renewable Energy Sources Act (EEG) intends to raise the share of renewable energies in gross electricity consumption to at least 80% by 2030. Along with other far-reaching political decisions to achieve this goal, an accelerated expansion of onshore and offshore wind energy is urgently needed and essential. This will have a significant impact not only on the future siting of wind turbines and the associated development of power grids, but also on many other areas of the electricity sector, creating an urgent need for further research.

National energy studies often include wind power generation using high spatial but low temporal resolutions, as in many different analyses of the German electricity sector [3,4]. There are also wind power simulations that already deliver a high temporal and spatial resolution for Germany [5,6], but do not yet contain data from offshore turbines.

Offshore wind energy has been strongly expanded in recent years, and is now an important factor for the German electricity supply [7]. Therefore, it should be included in future energy studies. In order to better understand the various impacts of a growing share of variable renewables and to optimize their further expansion [3,4,8,9], disaggregated data on wind power generation are becoming increasingly important. For example, energy studies targeting distributed variable renewables in a decentralized power system can benefit from such information to identify potential power shortages caused by local turbine outages or regional wind lulls [10]. The absence of disaggregated electricity data for a given geographic area and time period, e.g., due to restrictive German data privacy laws, makes it difficult for academia and industry to study the various impacts of wind turbines at local and regional levels. To overcome this gap, the paper presents a comprehensible approach for creating power generation data from onshore and offshore turbines with a high temporal and spatial resolution.

The remaining sections of this work are organized as follows: Section 2 describes the plant and weather data used, as well as the input data required to calibrate the simulation model and validate the results obtained. The simulation model, which is the next evolutionary step of our wind power model [11,12], and its implementation are presented in Section 3. In addition to a more accurate calculation of the atmospheric variables at the turbine hub height, this extended model now allows simulations for any onshore or offshore wind turbine in Europe, once its plant data are known. In Section 4, the simulation model is applied to ensembles of nearly 28,000 onshore and 1500 offshore turbines in Germany to simulate the wind power generation for 2019 and 2020. The time series obtained are spatially aggregated and then compared with measured feed-in data to validate the simulations performed. Section 5 uses these simulation results for an application example in which the wind power generation and associated indicators are shown at the federal state level (NUTS-1), where the abbreviation NUTS refers to the Nomenclature of Territorial Units for Statistics. Finally, the paper closes with a set of informative conclusions in Section 6.

## 2. Input Data

This section describes the input data needed for the simulations as well as their sources and characteristics. Figure 1 sketches the development scheme of the presented wind power model with all involved data from calibration to validation. In this scheme, the input and output data are represented by red and blue containers, respectively. The direction of the data flow is indicated by the arrows.

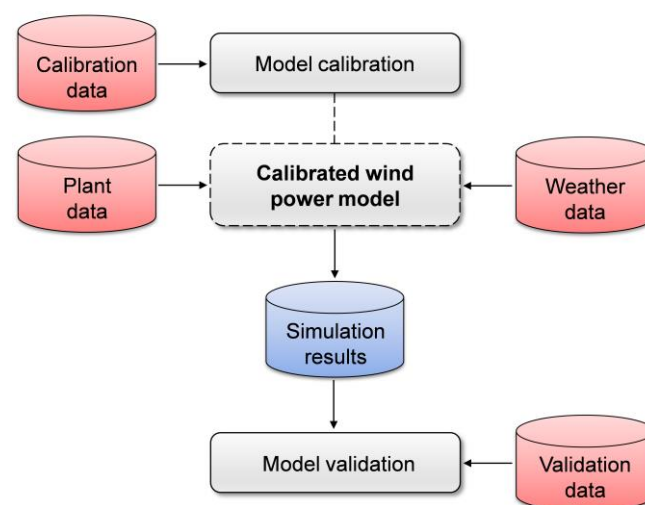


**Figure 1.** Development scheme of the wind power model with all involved data.

All of these input data, described in the following subsections, are publicly available, and allow a better understanding of the presented simulations and facilitate the development of other wind power models using the same or similar data sources.

### 2.1. Plant Data

The plant datasets used for the onshore and offshore turbines come from the open-access research data repository Zenodo (<https://doi.org/10.5281/zenodo.6922043> (accessed on 29 July 2022)). These datasets, which contain the wind turbines installed in Germany until 7 May 2021, were extracted from the Core Energy Market Data Register, as described in the related data paper [13]. According to this study, machine learning techniques were applied to the datasets in order to fill in missing technical parameters or to correct misplaced plant locations. After filtering both datasets for plants operating in the investigated years 2019 and 2020, the final ensembles of onshore and offshore turbines comprise the following data, as shown in Table 1.

**Table 1.** Ensemble data listed for each turbine ensemble and year.

Ensemble Data	Onshore Turbines		Offshore Turbines	
	2019	2020	2019	2020
Number of plants	27,532	27,873	1465	1497
Total capacity in MW	52,751	54,076	7545	7764
Total capacity in MW <sup>1</sup>	53,187	54,414	7555	7774

<sup>1</sup> Figures are from the Working Group on Renewable Energy Statistics (AGEE-Stat) [2].

The resulting installed capacity agrees well with the official German figures for 2019 and 2020, according to AGE-Stat [2]. In this context, the small deviations of less than 1% from the official values also confirm that most of the wind turbines receiving guaranteed feed-in tariffs under the EEG are included in the final datasets. Table 1 also shows that the expansion of installed capacity in the period from 2019 to 2020 is about 2.5% for onshore turbines and just under 3% for offshore turbines. This results in a total capacity increase for Germany of only 1.5 GW in this time period.

As known from previous energy studies [14–16], wind turbine datasets for large areas or whole countries are hardly complete due to the high number of single plants with many technical parameters. Therefore, it makes sense to use only the data that are absolutely necessary to perform the wind power simulations. For example, the presented wind power model does not require the rotor diameter of a wind turbine, so any uncertainties regarding this parameter are not able to influence the simulation results. This technical parameter is typically subject to inconsistencies [13] as the information provided by official sources on rotor diameter is often incomplete, or there is confusion between rotor radius and rotor diameter. For each wind turbine, the final datasets include the geographic location in latitude and longitude coordinates, rated power, hub height, turbine type, and date of (de)commissioning, as listed in Table 2.

**Table 2.** Plant data of the wind turbine datasets relevant for the numerical simulations.

Plant Data	Model Use
Latitude	mandatory
Longitude	mandatory
Rated power	mandatory
Hub height	mandatory
Turbine type	optional
Commission date	mandatory
Decommission date	optional

Since the turbine type is often only incompletely described or not available in the plant datasets used, the wind turbines are assigned to corresponding power classes with typical

power curves of common wind turbines. For example, the normalized power curve of an Enercon E-82 with 2050 kW is used in the simulation model for wind turbines with a rated power in the range of 1500 to 2500 kW. However, all other plant data listed in Table 2 are considered separately for each wind turbine. The different power classes with their power ranges and associated turbine types are shown in Table 3.

**Table 3.** Power classes with their ranges of rated power ( $P_R$ ) and associated turbine types.

Power Class in kW	Power Range in kW	Turbine Type
100	$P_R \leq 150$	Fuhrländer FL100
200	$150 < P_R \leq 250$	Enercon E-30
500	$250 < P_R \leq 750$	Enercon E-40
1000	$750 < P_R \leq 1500$	Vestas V52
2000	$1500 < P_R \leq 2500$	Enercon E-82
3000	$2500 < P_R \leq 3500$	Vestas V112
5000	$P_R > 3500$	Enercon E-126

## 2.2. Weather Data

Validated weather products play a key role in modeling the wind power generation, and their quality is essential for the accuracy of numerical simulations. For the European region, weather data with different temporal and spatial resolutions are freely accessible from numerous weather services worldwide via their web interfaces. Reanalysis weather products are a commonly used data source for studies on variable renewable energies, especially for wind power simulations [15–19]. Such reanalysis products are generated by using weather prediction models that are re-run for a specified period in the past and then corrected with measured weather information. MERRA and MERRA-2 reanalysis data, created by NASA’s Global Modeling and Assimilation Office with global coverage and a horizontal resolution of about 50 km [20,21], have become a de facto standard in many wind power simulations [18]. There are also several studies available for Germany using these weather data, e.g., a wind energy index study based on MERRA wind speeds [22]. Compared to the more recent ERA-5 reanalysis product, which has a higher spatial resolution of about 31 km and can therefore outperform MERRA [18], the improvements over MERRA-2 in terms of wind power generation for the German region are relatively small according to [19]. Furthermore, comprehensive wind power simulations for Europe in [23] show that a high correlation ( $R^2$ ) of more than 0.95 with historical data for Germany can be achieved with bias-corrected MERRA data.

This work uses MERRA-2 weather data provided by the freely accessible web tool of renewables.ninja ([www.renewables.ninja](http://www.renewables.ninja) (accessed on 23 January 2023)) [24], which delivers bias-corrected reanalysis data for Europe [23]. These weather data, which are retrieved separately for each turbine site using its geographic coordinates, have a temporal resolution of one hour. Using the renewables.ninja’s spatial interpolation feature reduces the number of web requests and avoids subsequent interpolations of the MERRA-2 reanalysis data. This significantly decreases the runtime of the simulations and the uncertainties caused by external interpolation routines. The time series, obtained by two web requests for a given time period and plant location, provide the following data for the wind power model: date and time in Coordinated Universal Time (UTC), air density at ground level, and wind speed at 50 m above the ground. Since the retrieved weather information is available for both onshore and offshore turbine sites, which is not the case for the weather product employed in our previous wind power simulations [6,12], the MERRA-2 weather data via the renewables.ninja web tool were used for all numerical simulations in this study. In addition, the simulations can now be performed for each country or offshore region in Europe using the same reanalysis product. This also improves the ability to combine and compare the simulated data since they are based on the same bias-corrected weather product.

### 2.3. Calibration and Validation Data

Further data are required for a meaningful calibration of the wind power model and a reliable validation of the simulation results. For the calibration of the presented model, the specific power curves of the used wind turbines with their characteristic cut-in speed, rated speed and power, and cut-out speed are necessary (Figure 2a). Such power curves are often available as a list of discrete values, which can usually be found in technical datasheets provided by wind turbine manufacturers or on various web platforms, e.g., [www.thewindpower.net](http://www.thewindpower.net) (accessed on 29 July 2022) [25]. They describe the relationship between the wind speed at hub height and the corresponding output power of a wind turbine operating at a standardized air density of  $1.225 \text{ kg/m}^3$ .

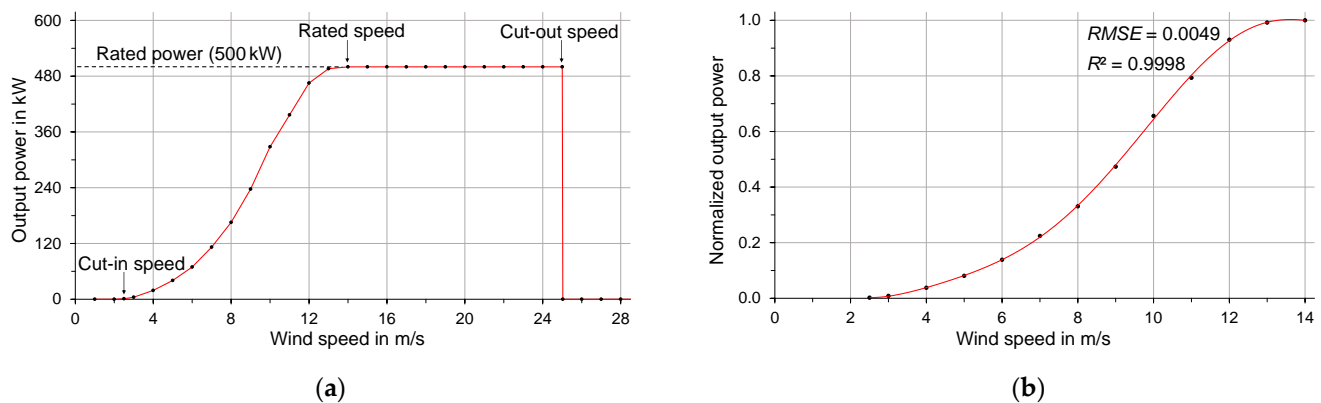


**Figure 2.** (a) Power curve (red line) of an Enercon E-40 as an example of a standard wind turbine. (b) Approximation of the nonlinear segment of the normalized E-40 power curve to a sixth-order polynomial (red line) with the associated  $RMSE$  and  $R^2$  values. The black dots on this curve mark the normalized values calculated from the discrete values of the manufacturer's datasheet [26].

The red line in Figure 2a depicts the specific power curve of a standard wind turbine, i.e., a pitch-controlled plant, with its technical parameters. Like the previous wind power model [12], the extended model uses sixth-order polynomial approximations for the power curves. As soon as an analytical representation is developed for a normalized power curve, the output power can be readily determined using the rated power of the wind turbine along with the wind speed and air density at its hub height. Figure 2b shows the approximated nonlinear segment of the normalized power curve from Figure 2a and the associated statistical measures, which also indicate the high accuracy of this modeling approach.

For additional power losses of wind turbines that are not included in the power curves, a further reduction of the output power has to be considered in the simulation model. These power losses are mainly caused by the following reasons:

1. Loss of power because of the wake effect (shading by other wind turbines);
2. Feed-in interruptions due to capacity constraints in the surrounding grids;
3. Plant shutdowns to overhaul wind turbines or to protect bats and birds;
4. Power reduction due to dirt or ice on the turbine rotor blades.

Since such data are not available for every single wind turbine, these kinds of power losses are considered in the wind power model as an averaged overall loss factor for the whole turbine ensemble. According to [27], this loss factor is typically between 5 and 30% for wind turbines at onshore sites. Moreover, offshore turbines experience further losses due to the larger distance from the onshore grid connection points and the additional converter platforms required. Such platforms convert the alternating current from offshore wind farms into direct current to reduce transmission losses to the mainland, but otherwise cause additional electrical losses in the conversion of electricity. Thus, the averaged overall loss factor is higher for offshore turbines, which must be taken into account for the simulations.

Meaningful average values for the turbine ensembles are also used for the Hellmann exponent, which is needed to extrapolate the wind speed to the hub height of the wind turbines using Hellmann's exponential law [28,29]. This Hellmann exponent or friction coefficient is a function of the topography at a given geographic location, taking into account the surface roughness. For onshore regions with a very heterogeneous topography of the plant locations, e.g., areas with hill or mountain ranges, the wind turbine ensemble can also be sorted into groups using different Hellmann exponents for the simulations to ensure a high degree of accuracy. The presented simulations for onshore turbines use the general value for open land, which fits well with the onshore sites of most wind power plants in Germany. For the offshore region, the value for lakes or sea is applied in the wind power model [29]. Table 4 shows the selected calibration data for onshore and offshore turbine ensembles. The values in this table have been shown in previous simulations to be realistic averages for turbine ensembles. In addition, the values listed for onshore turbines have already been used in peer-reviewed energy studies [6,12].

**Table 4.** Calibration data for onshore and offshore turbines needed for the wind power model.

Calibration Data	Onshore Turbines	Offshore Turbines
Loss factor in %	16	22
Friction coefficient	1/7	1/10

Furthermore, the results obtained from the wind power model have to be compared with measurements on real power systems to validate the simulations and to assess their accuracy. The presented simulation model is the next evolutionary step of our wind power model, which has already been validated with measurements of a technically known wind turbine [12]. Since the extended model includes modified calculations that only improve the accuracy of atmospheric variables at the turbine hub height, it is not practical to repeat the model validation with a single wind turbine using measured wind speeds at its hub height. Nevertheless, the numerical simulations shown in this paper consider large ensembles of onshore and offshore turbines. Therefore, the simulated data showing the power generation from these ensembles need to be checked against the measured feed-in time series. Since there is no publicly available information on wind power generation with a high spatial resolution, the simulated data cannot be validated at a highly resolved scale. However, if the simulation results are spatially summarized over Germany, they can be verified with measured feed-in time series for the whole of Germany. Such feed-in data are freely accessible via the SMARD web platform ([www.smard.de](http://www.smard.de) (accessed on 19 January 2022)) [30].

### 3. Simulation Model

This section introduces the wind power model, which is the next evolutionary step of our simulation model, presented in [11,12]. From a general perspective, data about wind power generation can be produced using either statistical [31] or physical models [15,19]. In contrast to statistical approaches such as vector autoregressive or Monte Carlo methods, as used in [31], the results of physical models are based on weather data obtained from extensive measurements or meteorological models. Thus, an advantage of physical models, such as the presented wind power model, is the ability to provide power generation data at a highly resolved temporal and spatial scale.

The data flows and calculation steps of the simulation model are depicted in Figure 3, where the plant and weather data are the input variables for the calibrated wind power model. The calculation steps are displayed as grey rectangles; all other symbols have the same meanings as in Figure 1.

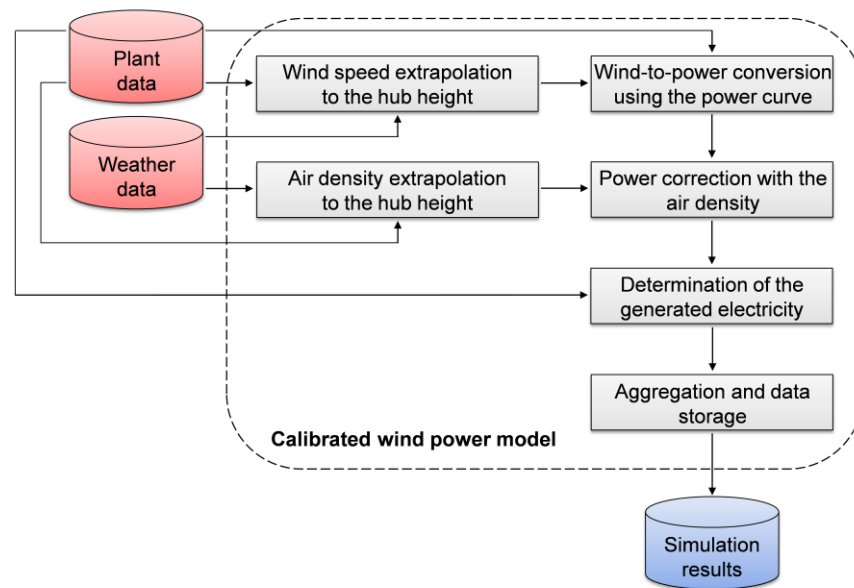


Figure 3. Structure of the simulation model with the data flows and calculation steps.

As mentioned in the previous subsection, the extended wind power model includes modified calculations that improve the accuracy of the atmospheric variables at the hub height of the wind turbines. For the necessary extrapolation of the wind speed to the required hub height, Hellmann's exponential law is used, which can be described by the following expression [28,29]:

$$v_H \approx \left( \frac{H_H}{H_0} \right)^\alpha \cdot v_0 \quad (1)$$

In this expression,  $v_H$  stands for the unknown wind speed at the turbine hub height  $H_H$  and  $v_0$  is the known wind speed at height  $H_0$  provided by the weather product. The exponent  $\alpha$  represents the Hellmann exponent. Unlike the previous simulation model, which uses wind speed data at 10 m above the ground, this wind power model operates with wind speeds at 50 m, which significantly improves the accuracy of the wind speed extrapolation to the hub height due to smaller height differences. For the air density, the other required atmospheric variable, the calculations have also been further improved in the presented wind power model. In contrast to the previous model, which estimates the air density at the turbine hub height using air pressure and temperature information, the extended model uses the air density data provided by the weather product. The necessary extrapolation of the air density to the required hub height is performed by the following approximation applying the barometric height formula:

$$\rho_H \approx \exp\left(-\frac{H_H}{H_S}\right) \cdot \rho_0 \quad (2)$$

In this formula,  $\rho_H$  denotes the unknown air density at the turbine hub height  $H_H$  and  $\rho_0$  is the air density at ground level provided by the weather data. The scale height  $H_S$  has a value of about 8430 m for an isothermal atmosphere of 288.15 K. As described in the previous subsection and shown in Figure 2b, the simulation model uses sixth-order polynomials for the normalized power curves of wind turbines. With this analytical representation of the power curve, the output power can be readily calculated for any intermediate wind speed, i.e., without the need for interpolations. This calculation step delivers the output power  $P_N$  at a standardized air density  $\rho_N$  of 1.225 kg/m<sup>3</sup>, which corresponds to an air temperature of 288.15 K at a normal atmospheric pressure of 1.013 bar.

Therefore, the output power value obtained must be corrected with the actual air density at the turbine hub height using the power correction relationship given in [32]:

$$P_C \approx \left( \frac{\rho_H}{\rho_N} \right) \cdot P_N \quad (3)$$

In this relationship,  $P_C$  represents the corrected output power using the air density at the hub height of the wind turbine. The next step is to calculate the produced electricity by multiplying the corrected output power with the time window provided by the temporal resolution of the weather product. In the case of MERRA data, this is an hourly resolution. In this calculation step, additional turbine losses and the date of (de)commissioning of the wind turbines are also taken into account in order to include power losses not covered by the power curve, as well as possible plant changes in the considered time period. Finally, the resulting hourly resolved time series is converted from UTC to local time and, if necessary, aggregated to another time series, e.g., with a daily resolution. After the calculation steps, as shown in Figure 3, have been performed for all wind turbines of the plant dataset, the time series are stored as comma-separated values.

#### 4. Simulation Results

The following subsections present the results obtained with the previously described input data and the extended wind power model. The simulated and spatially aggregated time series of the turbine ensembles are compared with the measured feed-in data for all of Germany in order to validate the simulations and to discuss the reasons for the existing deviations.

##### 4.1. Onshore Turbine Ensemble

The presented simulation model was used to determine the power generation from onshore wind turbines in Germany for the years 2019 and 2020. After model validation using measurements of a technically known wind turbine [12], the numerical simulations were performed with an ensemble of 27,532 onshore turbines for 2019 and 27,873 onshore turbines for 2020, as presented in Table 1. For this purpose, each wind turbine of the used plant datasets was simulated separately, and the MERRA-2 reanalysis data were retrieved via the renewables.ninja web tool for each turbine site. According to Table 4, an overall loss factor of 16% and a Hellmann coefficient of 1/7 was applied to the entire onshore turbine ensemble. After performing the simulations, the hourly resolved time series were transformed into a time series for each year to verify the obtained results with measured feed-in data for all of Germany. To facilitate this verification, the measured and simulated time series were converted from an hourly to a daily resolution, as displayed in Figure 4.

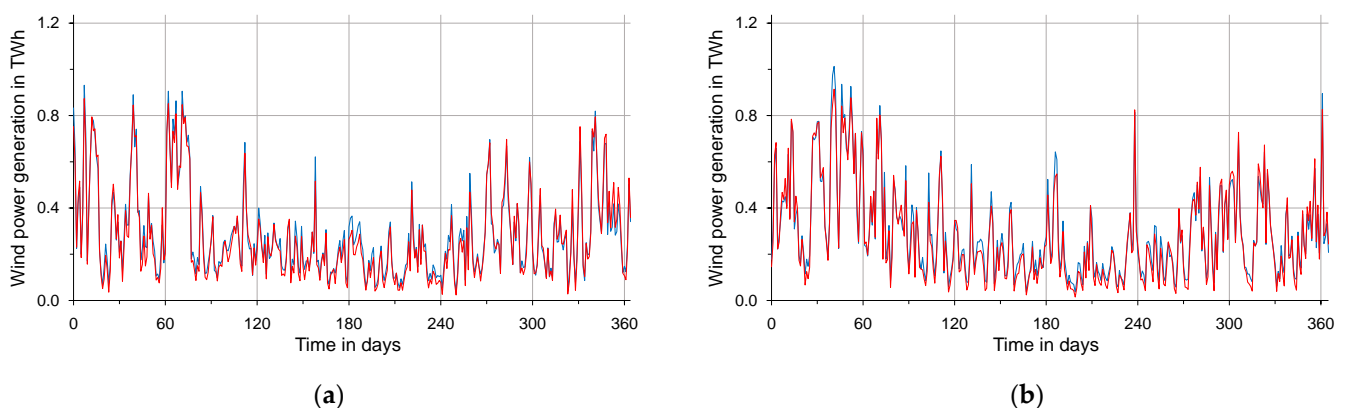


**Figure 4.** Measured feed-in time series (red line) and simulated wind power generation (blue line) from onshore turbines in Germany for the years (a) 2019 and (b) 2020 with a daily resolution.

As shown in Figure 4, the simulated wind power generation is in good agreement with the measured feed-in time series for the entire period from 2019 to 2020. It can also be seen that most of the electricity is produced in the winter months, which is typical for wind turbines located in onshore regions. The small deviations between the measured and simulated time series are mainly due to the following reasons, which are not covered by the presented simulation model:

1. Deviations due to the interpolation of the weather data to the turbine sites;
2. The use of an averaged overall loss factor for the turbine ensembles;
3. The assignment of wind turbines to corresponding power classes;
4. Deviations due to the use of hourly averaged wind speed data.

For an additional verification at a small spatial scale, we compared the simulation results with annual values at the NUTS-1 level. The city-state of Hamburg was chosen because it covers a small geographic area and provides official values for the power generation from onshore turbines for the years 2019 and 2020. Table 5 shows the simulated and official values, as well as the ratio of official to simulated values as a relative measure of the existing deviations.

**Table 5.** Annual power generation from onshore turbines in the city-state of Hamburg.

Power Generation	2019	2020
Simulated value in GWh	256	257
Official value in GWh <sup>1</sup>	237	236
Deviation in %	7.4	8.2

<sup>1</sup> Figures are from the Statistisches Amt für Hamburg und Schleswig-Holstein [33].

These deviations in the single-digit percentage range indicate that the simulations also provide sufficiently accurate results even at small spatial scales with a low number of wind power plants.

#### 4.2. Offshore Turbine Ensemble

The offshore wind turbines were simulated in the same way as the onshore turbine ensemble, i.e., using the input data previously described and the calibration values for offshore turbines from Table 4. After running the numerical simulations for an ensemble of 1465 offshore turbines for 2019 and 1497 offshore turbines for 2020, the hourly resolved data were transformed into a time series for each year to compare the simulation results with measured feed-in data of all German offshore turbines. The measured and simulated time series, also transformed to a daily resolution, are depicted in Figure 5.

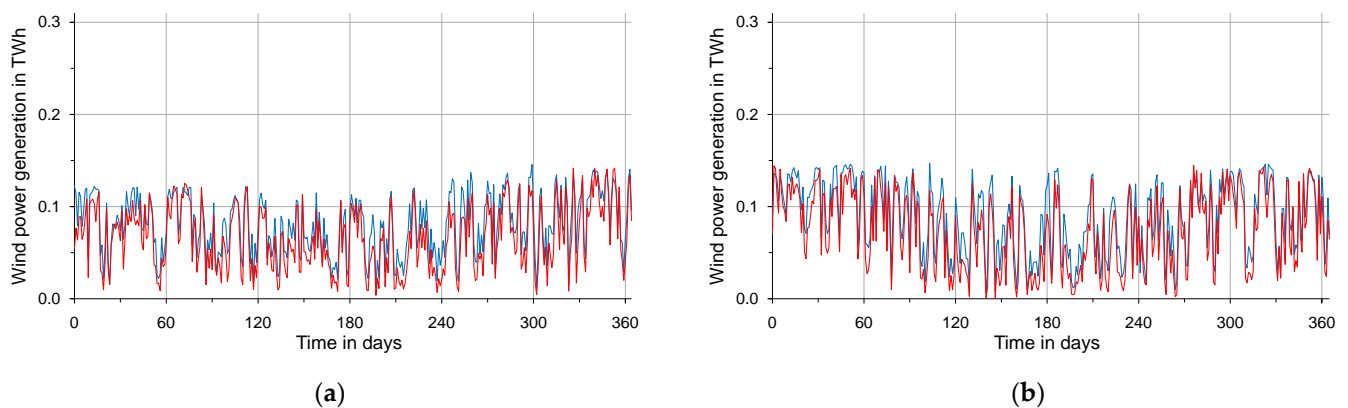


**Figure 5.** Measured feed-in time series (red line) and simulated wind power generation (blue line) from offshore turbines in Germany for the years (a) 2019 and (b) 2020 with a daily resolution.

Figure 5 shows that our wind power model reproduces well the pattern of the measured time series for both annual periods. Compared to onshore sites, the offshore wind power generation is more constant throughout the year due to the more stable wind conditions at sea. The existing deviations between the measured and simulated time series are caused by the same reasons as already described for the simulation results of the onshore turbines. In addition, the often-higher values from the simulations may indicate a higher number of feed-in interruptions for offshore turbines due to capacity constraints in the surrounding, insufficiently developed mainland grids.

#### 4.3. Validation of the Simulations

In order to verify the simulation results not only visually with measured feed-in data, additional statistical measures were applied to numerically assess the quality of the simulations. For this purpose, the Root-Mean-Square Error (*RMSE*) and the Mean Absolute Error (*MAE*) were determined for the time series to identify the differences between the measured and simulated data. Furthermore, the *RMSE* and *MAE* can also be set in relation to the total feed-in  $F_{\text{tot}}$  in order to indicate the relative deviations. These relative statistical measures can be described by the following equations:

$$RMSE_{\text{rel}} = \sqrt{\frac{1}{n \cdot F_{\text{tot}}^2} \sum_{i=1}^n (x_i - y_i)^2} \quad (4)$$

$$MAE_{\text{rel}} = \frac{1}{n \cdot F_{\text{tot}}} \sum_{i=1}^n |x_i - y_i| \quad (5)$$

In both equations,  $x_i$  and  $y_i$  represent the daily values of the measured and simulated time series of length  $n$ . As a deeper statistical evaluation, a Pearson correlation between the first differences of the measured and simulated time series was determined according to the following relationship [6]:

$$R_{XY} = \frac{\sum_{i=1}^{n-1} (X_i - X_m) \cdot (Y_i - Y_m)}{\sqrt{\sum_{i=1}^{n-1} (X_i - X_m)^2 \cdot \sum_{i=1}^{n-1} (Y_i - Y_m)^2}} \quad (6)$$

In this relationship,  $R_{XY}$  stands for the correlation coefficient,  $X_i$  and  $Y_i$  are the first differences for the daily values of the measured and simulated time series of length  $n$ , and  $X_m$  and  $Y_m$  are the corresponding mean values. Table 6 shows the measured total feed-in and the statistical measures of the simulation results for each turbine ensemble and year.

**Table 6.** Total feed-in ( $F_{\text{tot}}$ ) and statistical measures for each turbine ensemble and year.

Ensemble Measures	Onshore Turbines		Offshore Turbines	
	2019	2020	2019	2020
$F_{\text{tot}}$ in TWh	99.6	103.1	24.2	26.9
<i>RMSE</i> in GWh	32.9	33.9	18.5	19.9
<i>RMSE</i> <sub>rel</sub> in %	0.03	0.03	0.08	0.07
<i>MAE</i> in GWh	26.9	27.6	16.0	17.3
<i>MAE</i> <sub>rel</sub> in %	0.03	0.03	0.07	0.06
$R_{XY}$	0.98	0.98	0.94	0.94

The calculated statistical measures in this table confirm that the simulation results are in good agreement with the measured feed-in data for all of Germany. The relative *RMSE* and *MAE* values in the range of 0.03 to 0.08% underline this agreement. Moreover, correlation coefficients of 0.98 for onshore turbines and 0.94 for offshore turbines indicate that the trends of the measured and simulated time series vary in the same direction and magnitude. In addition, the obtained statistical measures show comparably low or partly lower deviations compared to previous wind power simulations for the year 2016 [6,12],

which employed satellite-based weather data with even a higher horizontal resolution. This reveals another advantage of our wind power model over simulation models that use only wind speed data as an atmospheric variable [34,35], because it also incorporates air density data from the same weather product to correct the output power provided by the power curve, resulting in more accurate simulations. Thus, the obtained results can be used to determine the power generation from wind turbines at different spatial scales for Germany.

### 5. Application Example

Local and regional advances in the transformation of the electricity sector towards a higher share of wind energy can be reliably tracked by the spatiotemporal distribution of wind turbines and their power generation. Thus, the simulation results generated in this study may help to better monitor the German energy transition. As an example of application at the regional scale, Figure 6 shows the power generation from offshore turbines and onshore turbines at NUTS-1 level with a daily resolution. Particularly at this spatial level, many political decisions and regulations are made in Germany which have a major impact on the decarbonization of the energy system and the speed of its implementation.

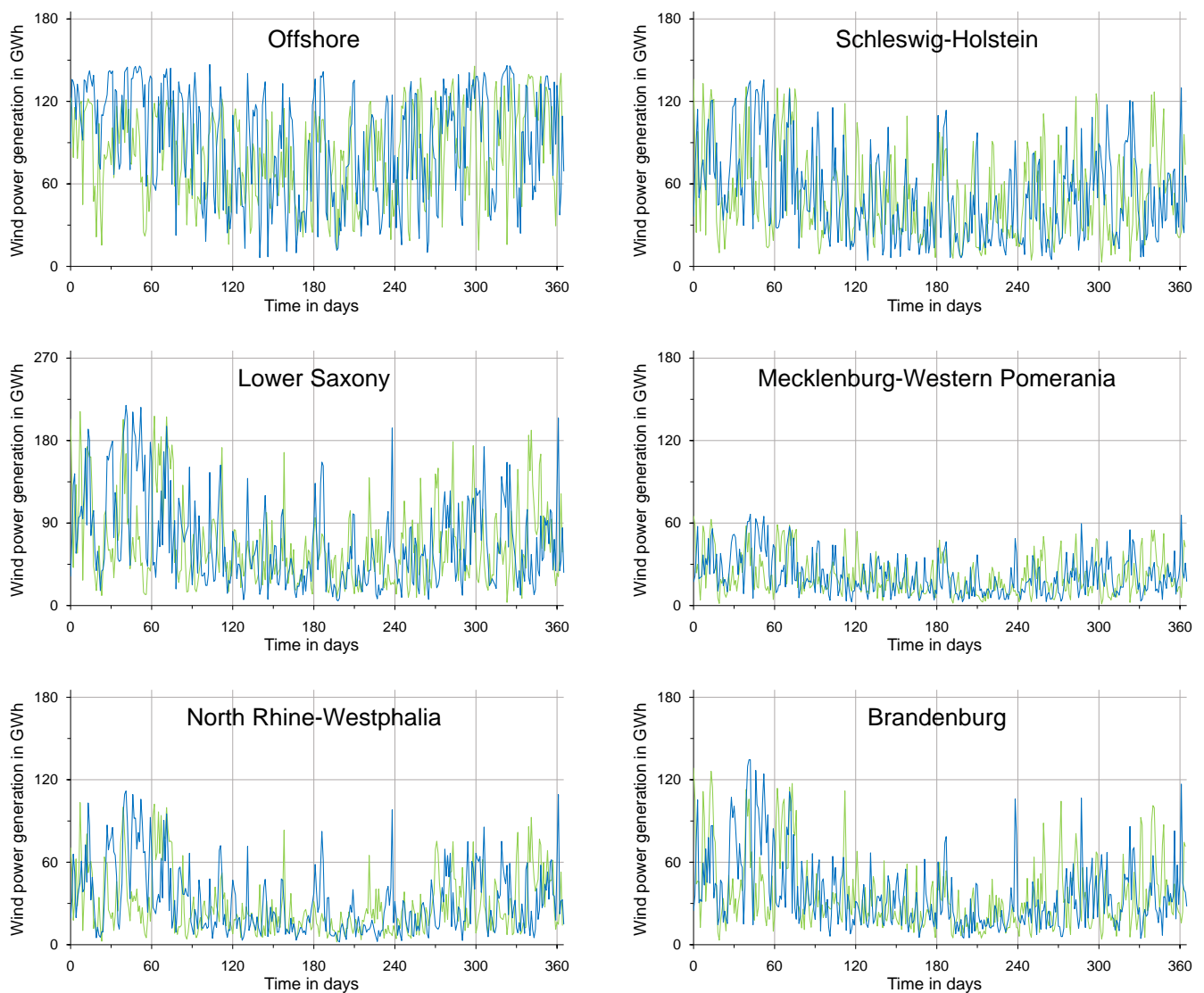
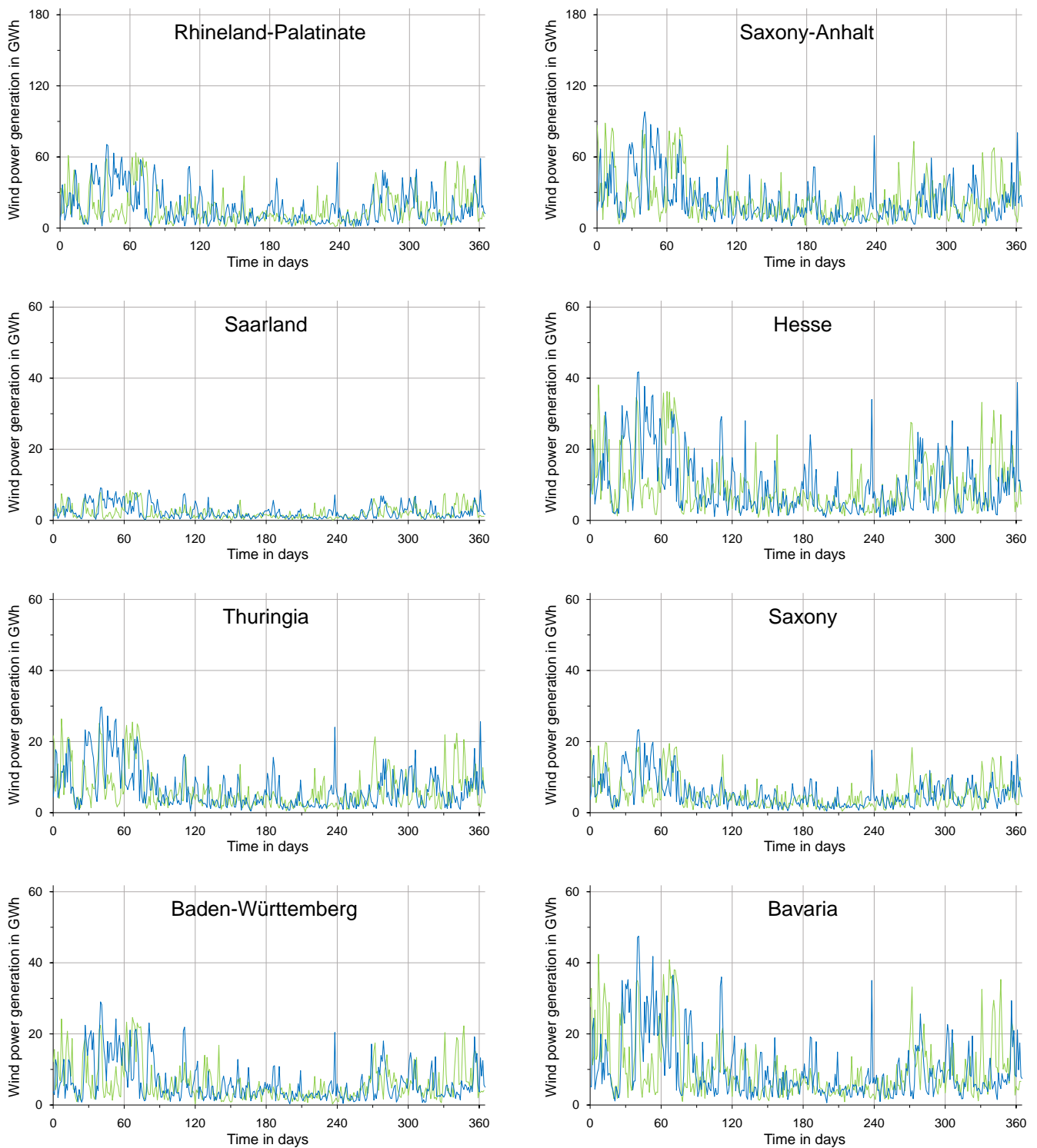


Figure 6. Cont.



**Figure 6.** Aggregated wind power generation from offshore turbines and onshore turbines at NUTS-1 level in Germany for the years 2019 (green line) and 2020 (blue line) with a daily resolution. The city-states Bremen, Hamburg, and Berlin are not included due to the low number of wind power plants.

From the time series in Figure 6, it is easy to see that power generation from onshore turbines is much higher in the northern states, such as Schleswig-Holstein, Lower Saxony, and Brandenburg, than in the southern states, such as Saxony, Saarland, and Baden-Württemberg, even though the latter is the third largest federal state in terms of area. It can also be seen for the investigated years 2019 and 2020 that onshore sites typically generate

more wind power from October to March than in the other months, especially in inland states such as North Rhine-Westphalia, Thuringia, and Bavaria. As already mentioned in the previous section, the offshore wind power generation is more constant throughout the year due to the more stable wind conditions at sea. This is also partly the case in federal states with a high proportion of coastal areas, such as Schleswig-Holstein and Mecklenburg-Western Pomerania.

The simulated power generation can be also related to the installed capacity of the wind turbines in order to determine their efficiency depending on the geographic area and time period under investigation. Moreover, the installed capacity can be set in relation to the investigated area to have a comparable indicator of how far this region is in terms of wind energy deployment. For this purpose, a spatiotemporal capacity density  $CD_{st}$  and capacity factor  $CF_{st}$  can be defined according to the following equations:

$$CD_{st} = \frac{C_{wt}}{A} \quad (7)$$

$$CF_{st} = \frac{E_{wt}}{T \cdot C_{wt}} \times 100\% \quad (8)$$

In these equations,  $C_{wt}$  represents the wind turbine capacity installed in the investigated area  $A$ ,  $T$  stands for the investigated time period, and  $E_{wt}$  is the generated electricity from wind turbines in this area and period. Table 7 provides the capacity density and the capacity factor at NUTS-1 level in Germany for the years 2019 and 2020.

**Table 7.** Capacity density ( $CD_{st}$ ) and capacity factor ( $CF_{st}$ ) at NUTS-1 level for 2019 and 2020.

Offshore/Federal State	$CD_{st}$ in kW/km <sup>2</sup>		$CF_{st}$ in %	
	2019	2020	2019	2020
Offshore	-	-	45.1	48.4
Schleswig-Holstein	425	433	31.8	31.7
Mecklenburg-Western Pomerania	144	147	26.8	26.6
Bremen	475	475	25.9	26.5
Lower Saxony	232	235	25.1	25.8
Hamburg	161	161	24.1	24.2
North Rhine-Westphalia	169	178	20.9	21.8
Berlin	14	14	22.9	22.6
Brandenburg	244	252	20.7	20.5
Rhineland-Palatinate	185	188	18.6	20.0
Saxony-Anhalt	251	256	19.1	18.6
Saarland	185	196	19.2	20.3
Hesse	103	107	18.7	18.9
Thuringia	98	101	17.3	17.4
Saxony	68	69	17.5	17.6
Baden-Württemberg	43	44	16.6	17.0
Bavaria	35	36	16.9	16.7
Onshore	148	151	22.6	22.9

Table 7 shows that the increase in capacity density, and therefore installed capacity, between 2019 and 2020 is small in all federal states. Some states, such as Saxony, Baden-Württemberg and Bavaria, show very little growth or, like the three city-states, no growth at all. The federal states with the lowest values of capacity density, excluding Berlin, are also Saxony, Baden-Württemberg, and Bavaria, i.e., there is a large untapped potential for wind energy in these regions. These three states are also well below the average onshore value in Germany, which increases from 148 to 151 kW/km<sup>2</sup> in this time period. The capacity factors show that the values are highest for offshore turbines, with 45% in 2019 and 48% in 2020, and also for federal states with a high proportion of coastal areas. For example, Schleswig-Holstein achieves a capacity factor of 32% and Mecklenburg-Western

Pomerania of 27% in the time period considered. In contrast, the states in the far south, such as Baden-Württemberg and Bavaria, only reach values of 17%, also due to the poorer wind conditions there. The average onshore capacity factor for the whole of Germany is 23% for 2019 and 2020.

Since each wind turbine is simulated separately with its geographic location and technical parameters, the power generation can also be represented at any other spatial scale, e.g., at the county level, which has already been shown for the year 2016 using the previous wind power model [6].

## 6. Conclusions

The main motivation for this study was to obtain high-resolution electricity data of wind turbines in Germany, which are currently not publicly available to academia and industry due to restrictive German data privacy laws. The years 2019 and 2020 were chosen because, at the time of writing this paper, the plant and weather data applied were only fully available until the end of 2020. Another reason for using this time period is the continuation of the energy transition analysis of the German electricity sector [3,6], including power generation data of onshore and offshore turbines for 2019 and 2020.

This work presents a comprehensible approach for generating highly resolved power generation data of wind turbines using numerical simulations. In order to support such an approach, the necessary input variables, i.e., the plant and weather data, should be publicly available, so that potential users can develop their own wind power model based on the ideas presented. The simulations in Section 4 clearly show that the wind power model can be used to generate sufficiently accurate electricity data for large onshore and offshore turbine ensembles. For the simulation of the wind power generation in Germany for the years 2019 and 2020, nearly 28,000 onshore and 1500 offshore turbines were considered. The resulting time series have a spatial resolution at the turbine site level and reach an hourly time resolution based on the weather product. To the best of our knowledge, such high-resolution power generation data for 2019 and 2020, taking into account almost all wind turbines in Germany that receive guaranteed feed-in tariffs under the EEG, have never been reported before. These simulation results can also serve as a basis for modeling optimal transformation paths of the German energy system with the help of scenario calculations using the numerical model described in [36,37]. In addition, the wind power model presented in this paper can be used for any country or offshore region in Europe, if the required plant data are available for these geographic areas.

Furthermore, the increasing share of variable renewable energies in the electricity sector requires additional efforts to ensure an optimal use of flexible renewables, such as biogas power plants [38]. Thus, the presented wind power model in combination with the photovoltaic model introduced in [39] can also help to optimize the local and regional demand for flexible power generation in order to better balance the fluctuating power from wind turbines and photovoltaic systems. Many other scientific studies can benefit from the power generation data provided by the simulation model for a given geographic area and time period, such as the influence of wind turbine noise on seismic recordings [40] or the effects of climate change on variable renewables [41].

**Author Contributions:** Conceptualization, R.L.; Methodology, R.L.; Software, R.L.; Validation, R.L.; Formal Analysis, R.L. and D.T.; Investigation, R.L.; Resources, R.L.; Data Curation, R.L.; Writing—Original Draft Preparation, R.L.; Writing—Review and Editing, R.L. and D.T.; Visualization, R.L.; Supervision, R.L. and D.T.; Project Administration, D.T.; All authors have read and agreed to the published version of the manuscript.

**Funding:** This research received general funding from the Helmholtz Association of German Research Centres.

**Data Availability Statement:** Not applicable.

**Conflicts of Interest:** The authors declare no conflict of interest.

## References

1. GWEC. *Global Wind Report 2022*; Global Wind Energy Council: Brussels, Belgium, 2022.
2. BMWK Zeitreihen zur Entwicklung der Erneuerbaren Energien in Deutschland unter Verwendung von Daten der Arbeitsgruppe Erneuerbare Energien-Statistik (AGEE-Stat). Available online: <https://www.erneuerbare-energien.de> (accessed on 14 November 2022).
3. Rauner, S.; Eichhorn, M.; Thrän, D. The spatial dimension of the power system: Investigating hot spots of Smart Renewable Power Provision. *Appl. Energy* **2016**, *184*, 1038–1050. [[CrossRef](#)]
4. Becker, R.; Thrän, D. Optimal Siting of Wind Farms in Wind Energy Dominated Power Systems. *Energies* **2018**, *11*, 978. [[CrossRef](#)]
5. Engelhorn, T.; Müsgens, F. How to estimate wind-turbine infeed with incomplete stock data: A general framework with an application to turbine-specific market values in Germany. *Energy Econ.* **2018**, *72*, 542–557. [[CrossRef](#)]
6. Lehneis, R.; Manske, D.; Schinkel, B.; Thrän, D. Spatiotemporal Modeling of the Electricity Production from Variable Renewable Energies in Germany. *ISPRS Int. J. Geo-Inf.* **2022**, *11*, 90. [[CrossRef](#)]
7. BMWK. Die Energiewende, Erneuerbare Energien 2021, Daten der Arbeitsgruppe Erneuerbare Energien-Statistik (AGEE-Stat). Available online: <https://www.erneuerbare-energien.de> (accessed on 21 September 2022).
8. Ramirez Camargo, L.; Stoeglehner, G. Spatiotemporal modelling for integrated spatial and energy planning. *Energy Sustain. Soc.* **2018**, *8*, 32. [[CrossRef](#)]
9. Yasuda, Y.; Carlini, E.M.; Estanqueiro, A.; Eriksen, P.B.; Flynn, D.; Herre, L.F.; Hodge, B.-M.; Holttinen, H.; Koivisto, M.J.; Gómez-Lózar, E.; et al. Flexibility chart 2.0: An accessible visual tool to evaluate flexibility resources in power systems. *Renew. Sustain. Energy Rev.* **2023**, *174*, 113116. [[CrossRef](#)]
10. Ottenburger, S.S.; Çakmak, H.K.; Jakob, W.; Blattmann, A.; Trybushnyi, D.; Raskob, W.; Kühnapfel, U.; Hagenmeyer, V. A novel optimization method for urban resilient and fair power distribution preventing critical network states. *Int. J. Crit. Infrastruct. Prot.* **2020**, *29*, 100354. [[CrossRef](#)]
11. Lehneis, R.; Manske, D.; Schinkel, B.; Thrän, D. Modeling of the power generation from wind turbines with high spatial and temporal resolution. In Proceedings of the 22nd EGU General Assembly, Online, 4–8 May 2020. [[CrossRef](#)]
12. Lehneis, R.; Manske, D.; Thrän, D. Modeling of the German Wind Power Production with High Spatiotemporal Resolution. *ISPRS Int. J. Geo-Inf.* **2021**, *10*, 104. [[CrossRef](#)]
13. Manske, D.; Grosch, L.; Schmiedt, J.; Mittelstädt, N.; Thrän, D. Geo-Locations and System Data of Renewable Energy Installations in Germany. *Data* **2022**, *7*, 128. [[CrossRef](#)]
14. Becker, R.; Thrän, D. Completion of wind turbine data sets for wind integration studies applying random forests and k-nearest neighbors. *Appl. Energy* **2017**, *208*, 252–262. [[CrossRef](#)]
15. Olauson, J.; Bergkvist, M. Modelling the Swedish wind power production using MERRA reanalysis data. *Renew. Energy* **2015**, *76*, 717–725. [[CrossRef](#)]
16. Cannon, D.J.; Brayshaw, D.J.; Methven, J.; Coker, P.J.; Lenaghan, D. Using reanalysis data to quantify extreme wind power generation statistics: A 33 year case study in Great Britain. *Renew. Energy* **2015**, *75*, 767–778. [[CrossRef](#)]
17. González-Aparicio, I.; Monforti, F.; Volker, P.; Zucker, A.; Careri, F.; Huld, T.; Badger, J. Simulating European wind power generation applying statistical downscaling to reanalysis data. *Appl. Energy* **2017**, *199*, 155–168. [[CrossRef](#)]
18. Gruber, K.; Regner, P.; Wehrle, S.; Zeyringer, M.; Schmidt, J. Towards global validation of wind power simulations: A multi-country assessment of wind power simulation from MERRA-2 and ERA-5 reanalyses bias-corrected with the global wind atlas. *Energy* **2022**, *238*, 121520. [[CrossRef](#)]
19. Olauson, J. ERA5: The new champion of wind power modelling? *Renew. Energy* **2018**, *126*, 322–331. [[CrossRef](#)]
20. Rienecker, M.M.; Suarez, M.J.; Gelaro, R.; Todling, R.; Bacmeister, J.; Liu, E.; Bosilovich, M.G.; Schubert, S.D.; Takacs, L.; Kim, G.-K.; et al. MERRA: NASA's Modern-Era Retrospective Analysis for Research and Applications. *J. Clim.* **2011**, *24*, 3624–3648. [[CrossRef](#)]
21. Gelaro, R.; McCarty, W.; Suárez, M.J.; Todling, R.; Molod, A.; Takacs, L.; Randles, C.A.; Darmenov, A.; Bosilovich, M.G.; Reichle, R.; et al. The Modern-Era Retrospective Analysis for Research and Applications, Version 2 (MERRA-2). *J. Clim.* **2017**, *30*, 5419–5454. [[CrossRef](#)]
22. Ritter, M.; Deckert, L. Site assessment, turbine selection, and local feed-in tariffs through the wind energy index. *Appl. Energy* **2017**, *185*, 1087–1099. [[CrossRef](#)]
23. Staffell, I.; Pfenninger, S. Using Bias-Corrected Reanalysis to Simulate Current and Future Wind Power Output. *Energy* **2016**, *114*, 1224–1239. [[CrossRef](#)]
24. Pfenninger, S.; Staffell, I. Renewables. Ninja. Available online: <https://www.renewables.ninja/> (accessed on 23 January 2023).
25. Pierrot, M. The Wind Power. Available online: <https://www.thewindpower.net/> (accessed on 29 July 2022).
26. ENERCON GmbH. *Datasheet ENERCON E-40/5.40*; ENERCON GmbH: Aurich, Germany, 2003.
27. Krebs, H.; Kuntzsch, J. Betriebserfahrungen mit Windkraftanlagen auf Komplexen Binnenlandstandorten. *Erneuerbare Energ.* **2000**, *12*, 2000.
28. Bañuelos-Ruedas, F.; Angeles-Camacho, C.; Rios-Marcuello, S. Methodologies Used in the Extrapolation of Wind Speed Data at Different Heights and Its Impact in the Wind Energy Resource Assessment in a Region. In *Wind Farm—Technical Regulations, Potential Estimation and Siting Assessment*; BoD—Books on Demand: Norderstedt, Germany, 2011. [[CrossRef](#)]
29. Petersen, E.L.; Mortensen, N.G.; Landberg, L.; Højstrup, J.; Frank, H.P. Wind Power Meteorology. Part I: Climate and Turbulence. *Wind Energy* **1998**, *1*, 2–22. [[CrossRef](#)]

30. SMARD—Strommarktdaten, Stromhandel und Stromerzeugung in Deutschland. Available online: <https://www.smard.de/home/> (accessed on 19 January 2022).
31. Ekström, J.; Koivisto, M.; Mellin, I.; Millar, R.J.; Lehtonen, M. A Statistical Modeling Methodology for Long-Term Wind Generation and Power Ramp Simulations in New Generation Locations. *Energies* **2018**, *11*, 2442. [[CrossRef](#)]
32. DIN EN 61400-12-1 VDE 0127-12-1:2017-12 Windenergieanlagen. Available online: <https://www.beuth.de/de/norm/din-en-61400-12-1/279191705> (accessed on 5 March 2020).
33. Statistisches Amt für Hamburg und Schleswig-Holstein—Anstalt des Öffentlichen Rechts (Statistikamt Nord), Steckelhörn 12, 20457 Hamburg, Germany. Available online: <https://www.statistik-nord.de> (accessed on 28 March 2023).
34. Bosch, J.; Staffell, I.; Hawkes, A.D. Temporally-explicit and spatially-resolved global onshore wind energy potentials. *Energy* **2017**, *131*, 207–217. [[CrossRef](#)]
35. Bosch, J.; Staffell, I.; Hawkes, A.D. Temporally explicit and spatially resolved global offshore wind energy potentials. *Energy* **2018**, *163*, 766–781. [[CrossRef](#)]
36. Millinger, M.; Tafarte, P.; Jordan, M.; Hahn, A.; Meisel, K.; Thrän, D. Electrofuels from excess renewable electricity at high variable renewable shares: Cost, greenhouse gas abatement, carbon use and competition. *Sustain. Energy Fuels* **2021**, *5*, 828–843. [[CrossRef](#)]
37. Aliabadi, D.E.; Chan, K.; Jordan, M.; Millinger, M.; Thrän, D. Abandoning the Residual Load Duration Curve and Overcoming the Computational Challenge. In Proceedings of the 2022 Open Source Modelling and Simulation of Energy Systems (OSMSES), Aachen, Germany, 4–5 April 2022; pp. 1–6. [[CrossRef](#)]
38. Thrän, D.; Lenz, V.; Liebetrau, J.; Krautkremer, B.; Kneiske, T.; Dreher, A.; Wille-Haufmann, B.; Dahmen, M.; Shu, D.Y.; Bau, U.; et al. Flexibler Einsatz von KWK, BHKW und Biogas-Anlagen durch Informations- und Kommunikationstechnik. In *Die Energiewende—Smart und Digital: Jahrestagung 2018 des Forschungs Verbunds Erneuerbare Energien*; Forschungs Verbund Erneuerbare Energien (FVEE): Berlin, Germany, 2019; pp. 35–40.
39. Lehneis, R.; Manske, D.; Thrän, D. Generation of Spatiotemporally Resolved Power Production Data of PV Systems in Germany. *ISPRS Int. J. Geo Inform.* **2020**, *9*, 621. [[CrossRef](#)]
40. Estrella, H.F.; Korn, M.; Alberts, K. Analysis of the Influence of Wind Turbine Noise on Seismic Recordings at Two Wind Parks in Germany. *J. Geosci. Environ. Prot.* **2017**, *5*, 76–91. [[CrossRef](#)]
41. Lehneis, R.; Manske, D.; Schinkel, B.; Thrän, D. Power Generation from Variable Renewable Energies (VRE). *Helmholtz Climate Initiative; Final Report Phase 1*. Berlin, Germany, 2022; pp. 213–215. Available online: <https://www.helmholtz-klima.de/en/projects/publications> (accessed on 22 February 2023).

**Disclaimer/Publisher’s Note:** The statements, opinions and data contained in all publications are solely those of the individual author(s) and contributor(s) and not of MDPI and/or the editor(s). MDPI and/or the editor(s) disclaim responsibility for any injury to people or property resulting from any ideas, methods, instructions or products referred to in the content.